Water-Triggered Self-Healing Coatings of Hydrogen-Bonded Complexes for High Binding Affinity and Antioxidative Property

Yong Du, Wen-Ze Qiu, Zi Liang Wu, Peng-Fei Ren, Qiang Zheng, and Zhi-Kang Xu**

Recent years have witnessed the rapid developments of self-healing coatings because they can protect materials from diverse risks and are able to autonomously heal after being physically damaged. Here, a universal yet facile method is reported with high time and cost efficiency to fabricate transparent water-enabled self-healing coatings on various substrates by precipitating hydrogen-bonded tannic acid (TA)-polyethylene glycol (PEG) complexes in aqueous solution. The precipitated complexes coalesce to form uniform and transparent coatings on the substrates; after drying, mechanically robust coatings are obtained. TA endows such coatings with strong adhesion to a wide range of substrates and admirable antioxidant properties. Repeatable self-healing of the coatings is realized by simply exposing them to water or humid environment. Furthermore, these coatings can be readily erased by soaking them in basic solution, if needed.

1. Introduction

Self-healing materials have raised increasing attentions due to their capacities of autonomously repairing mechanical damages, which reduce the safety risk and replacement cost of materials.[1–10] Among these materials, self-healing coatings have the unique function to protect the substrate materials against mechanical damage and corrosion while keeping their bulk properties.[11] There are generally two kinds of self-healing coatings, i.e., the extrinsic and intrinsic. Classical extrinsic self-healing coatings contain microstructures with healing agents;[12–14] this method is applicable to various coating matrices, and the resulting coatings can heal without additional stimuli.[15] On the other hand, intrinsic self-healing coatings are based on physical or chemical repairing of the coating matrices, so that the coatings can repeatedly heal; this approach avoids the pre-embedding processes and problems in the compatibility of healing agents in extrinsic self-healing coatings[16,17] and has developed rapidly in recent years.[18–25] In general, external stimuli, such as UV–vis light irradiation,[18,19] heating,[20,21] or special chemical environments,[22,23] are required to trigger the healing process because the substance migration of coatings is hindered by the substrates.[26]

Among intrinsic self-healing coatings, water-enabled self-healing coatings are especially promising because the healing is accomplished by simply soaking the coatings in water or exposing them to moisture,[27–36] without using any special devices or chemicals. Lyon and co-workers[25,36] first developed hydrogel thin films/coatings on polydimethylsiloxane by layer-by-layer (LBL) assembly of submicrometer-sized polyanionic gel particles and linear polycations; these films can rapidly heal micrometer-sized defects after exposed to water. Subsequently, Sun and co-workers have fabricated various kinds of water-enabled self-healing coatings by LBL assembly of polyelectrolyte multilayers.[11,27–30] Up to now, all water-enabled self-healing coatings are prepared by LBL assembly.[11,24–36] This method is advantageous in easy preparation and fine control over the coating structures. However, pretreatment of the substrates is usually needed for the subsequent LBL assembly; the resulting coatings cannot bind tightly to different materials. In addition, it is time-consuming especially in fabricating micrometer-thick coatings which are required for efficient healing of severe damages[27] and compensation for the lost substance in the coatings.[30] Therefore, it is desirable to develop a universal approach with high time and cost efficiency to fabricate mechanically robust water-enabled self-healing coatings on a wide range of substrates.

Here we report a versatile yet facile method to fabricate water-enabled self-healing coatings on various substrates, by precipitating hydrogen-bonded complexes of tannic acid (TA) and polyethylene glycol (PEG) in aqueous solution. TA, a natural polyphenol, endows the coatings with high binding affinity to different substrates[37–43] and antioxidant capacities.[38,46] TAs associate with PEGs into stable micrometer-sized complexes through intermolecular hydrogen bond in neutral or acidic aqueous solution.[44,45] With addition of NaCl, these complexes rapidly precipitate onto substrates under gravity and coalesce with each other to generate uniform soft coatings via hydrogen bonding. After drying, the hydrogen-bonding will be enhanced to produce mechanically robust coatings with strong adhesion to different substrates. However, the coatings become soft and

Y. Du, W.-Z. Qiu, Prof. Z. L. Wu, Dr. P.-F. Ren, Prof. Q. Zheng, Prof. Z.-K. Xu
MOE Key Laboratory of Macromolecular Synthesis and Functionalization
Department of Polymer Science and Engineering
Zhejiang University
Hangzhou 310027, China
E-mail: wuziliang@zju.edu.cn; xuzk@zju.edu.cn

DOI: 10.1002/admi.201600167

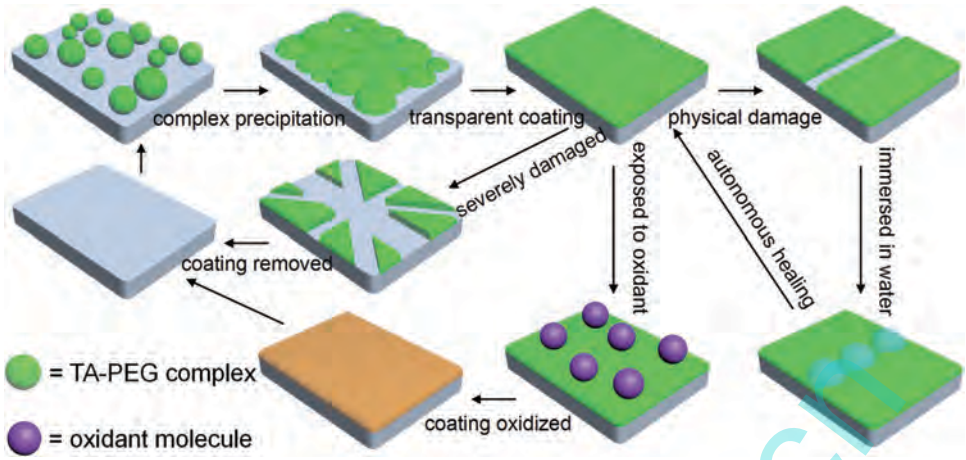

Scheme 1. Fabrication and multifunctions of TA-PEG water-enabled self-healing coatings on various substrates.

healable under water or in moist environment; they can rapidly and repeatedly repair micrometer-sized cuts. The TA-PEG coatings also show antioxidant properties because TA can capture reactive oxygen species (ROS).[38,46] To the best of our knowledge, this is the first self-healing coating having versatile properties, including repeatedly healing capacity, good transparency, high mechanical toughness, high binding affinity to various substrates, easy erasure on demand, and admirable antioxidant properties. Furthermore, our approach provides superior efficiency in time and cost, when compared to the traditional method, in fabricating water-enabled self-healing coatings. The facile fabrication and multifunctions of TA-PEG coatings are presented in **Scheme 1**. Such coatings should find applications in surface modification, material protection, and electronic packaging.

2. Results and Discussion

2.1. Fabrication of TA-PEG Coatings

The fabrication of TA-PEG coatings is schematically shown in **Figure 1**a. Typically, a polystyrene (PS) substrate was placed on the bottom of a 12-well plate (22 mm diameter); TA-PEG coatings were obtained by mixing TA and PEG aqueous solutions (each one 1.5 mL, 10 mg mL^{-1}, containing 0.5 M NaCl). TAs associate with PEGs to form stable, insoluble hydrogen bonded complexes with average diameter of ≈13 µm in NaCl aqueous solution (Figure S1, Supporting Information). The salt-free emulsion is stable without precipitation in 12 h (Figure S2, Supporting Information). Yet, in the presence of NaCl, which shields the negative charges of TA, the assemblies rapidly precipitate and coalesce with each other by hydrogen bonding on the bottom substrate to form a soft coating layer. The precipitation process is visualized as the whitish emulsion solution gradually becomes transparent (Figure S3, Supporting Information). The as-prepared coatings are transparent. Atomic force microscopy (AFM) reveals that the surface of such coatings is very smooth (Figure S4a, Supporting Information), indicating that the primary micrometer-sized complexes have coalesced to form a layer with a uniform structure. After drying, robust coatings are obtained.

Coating formation was observed in situ under an inverted optical microscope (Figure 1b). The bottom of a PS 12-well plate was directly used as the substrate for coating. At the beginning of precipitation, the horizon is uniform. In 3 min, several TA-PEG complexes precipitated on the substrate can be observed. Then, more and more complexes precipitate and start

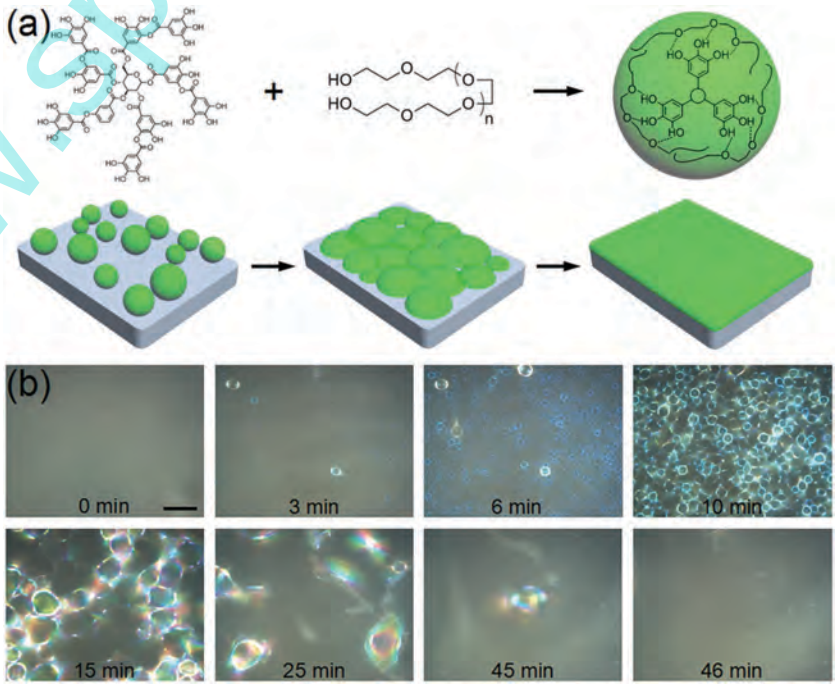

Figure 1. a) Scheme for the formation of TA-PEG hydrogen-bonded complexes and the fabrication of the coatings. b) Microscopic images to show the precipitating and coalescing process of TA-PEG complexes to form uniform coatings. Scale bar: 50 µm.

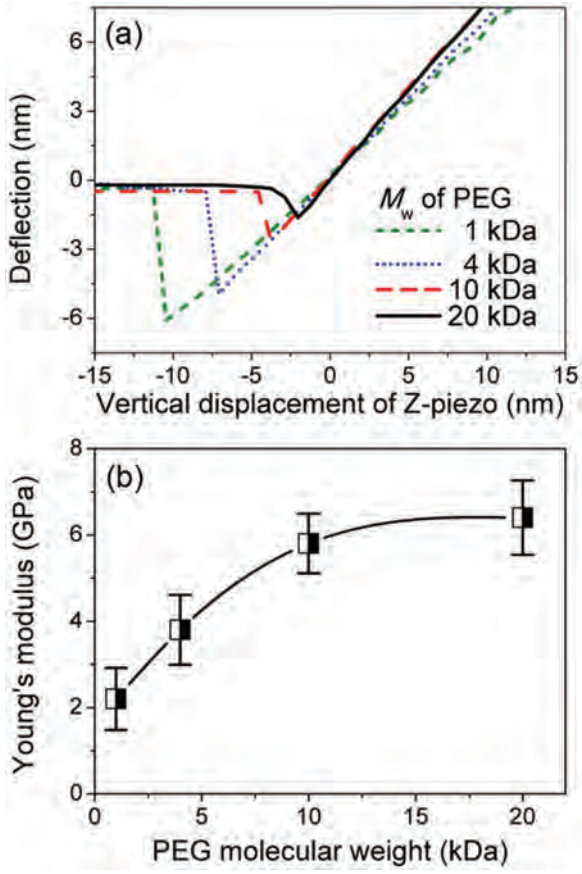

Figure 2. a) Deflection–displacement loading curves and b) corresponding Young's moduli of dry TA-PEG coatings composed of PEG with different molecular weights.

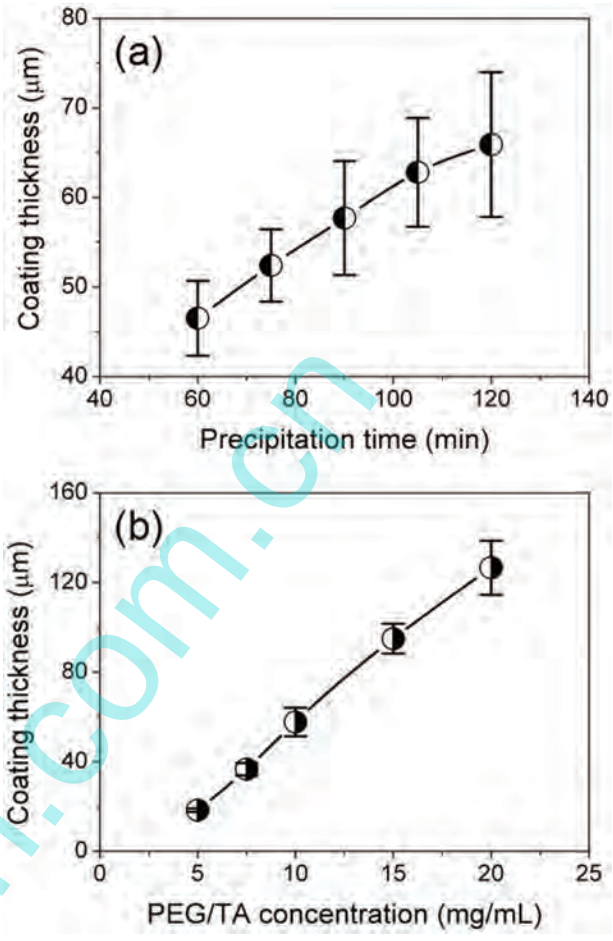

Figure 3. Thickness of TA-PEG coatings as a) a function of precipitation time and b) concentrations of TA and PEG. The concentrations of TA and PEG are fixed at 10 mg mL^{-1} in (a), whereas the precipitation time is fixed at 90 min in (b).

to coalesce. As a consequence, the complexes grow in size and spread to form a continuous coating. After 40 min, a uniform coating has already formed; yet complexes in the emulsion continue to precipitate and coalesce immediately with the preformed coating. During this process, the thickness of the coating gradually increases. At 45 min, we captured coincidentally the coalescing process of a large complex particle with the coating, which accomplishes within 1 s.

2.2. Optimal Condition and Tunable Thicknes

We investigated the effect of PEG molecular weight on the coatings. When the weight-average molecular weight, M_w, is 0.4 kDa, the mixed solution of PEG and TA in the presence of NaCl is totally transparent (Figure S5, Supporting Information), indicating that low molecular weight PEG cannot form complexes with TA. This is probably because the hydrogen-bond acceptor sites on PEG chains of low M_w are too few to form adequate intermolecular cross-linking with TA. When M_w of PEG is larger than 1 kDa, robust TA-PEG coatings can be obtained. However, their mechanical properties are different. By using AFM, Young's moduli (E) of the TA-PEG coatings are calculated from the indentation curves (**Figure 2**a).[47,48] E of coatings fabricated by using PEG with M_w of 1, 4, 10, and 20 kDa is 2.2, 3.8, 5.8, and 6.4 GPa, respectively. Figure 2b shows that E of the coatings increases significantly with M_w of PEG below 10 kDa; however, there is only slight increment when M_w of PEG varies from 10 to 20 kDa. In the systems with constant amount of TA and PEG, E should increase with the efficiency of TA-PEG intermolecular hydrogen bonding, which are related to the M_w of PEG. The increase in number of hydrogen bonding acceptors in each PEG molecule favors the formation of highly cross-linked structures. Therefore, in the following experiments we selected 20 kDa PEG to fabricate TA-PEG coatings with the most robust mechanical properties.

Then we studied the influence of TA/PEG ratio on the fabrication of TA-PEG coatings. Robust and uniform coatings are obtained when mass ratio (MR) of TA/PEG is 1. In contrast, when MR < 0.7, the hydrogen-bonded complexes are stable in the emulsion even with a high concentration of NaCl; no obvious precipitation occurs in 3 h to form the coating (Figure S6, Supporting Information). Thick PEG surface layer of the complexes might be the main hindrance to the precipitation and coalescence. However, when MR > 1.5, macroscopic cracks are found all over the coatings after drying

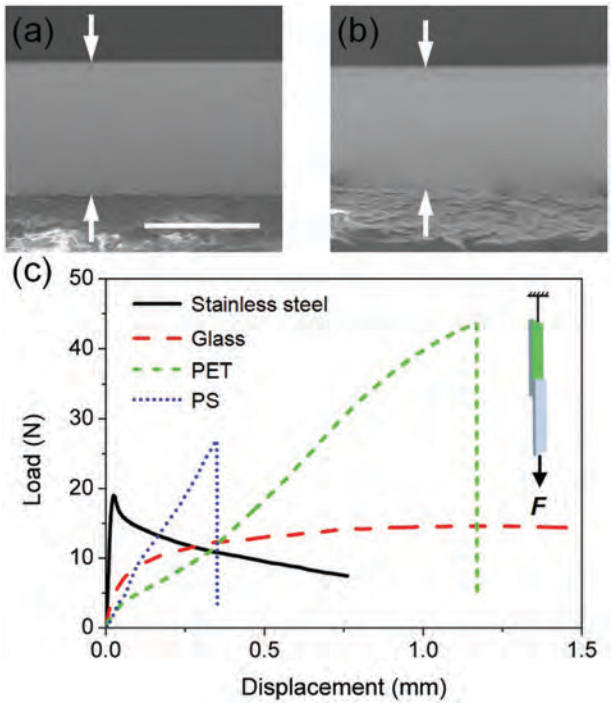

Figure 4. a,b) SEM images of TA-PEG coatings on PS substrates before (a) and after (b) peeled with an adhesive Scotch tape for ten times. Scale bar: 50 μm. d) Load–displacement curves for the adhesion of TA-PEG coatings to various substrates, measured by the lap shear tests. The area of coatings is 5×5 mm^2.

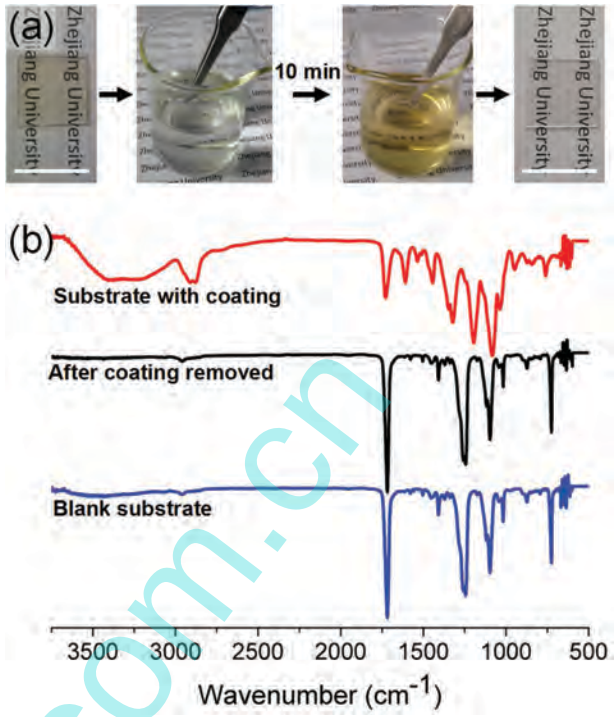

Figure 5. a) Digital images to show the erasure process of the TA-PEG coatings on PET substrates by soaking it in 0.01 M NaOH aqueous solution for 10 min. Scale bar: 1.5 cm. b) FT-IR/ATR spectra of the TA-PEG coatings before and after removed from the PET substrates. FT-IR/ATR spectrum of blank PET substrates is also shown for comparison.

(Figure S7, Supporting Information). The increase in the fraction of TA, a rigid molecule, results in the coatings to be fragile; therefore, drying leads to volume contraction and cracking of the coatings. In the following, MR of TA/PEG is kept as 1 to fabricate the coatings.

The thickness of TA-PEG coatings can be well controlled by tuning the fabrication conditions. The thickness is actually proportional to the total mass of complexes precipitated on the substrate per unit area. We can facilely fabricate coatings with well-defined thickness in tens of micrometers by tailoring the amount of complexes in the emulsion and the precipitation time. The thickness (T) of coatings after drying was measured by a scanning electron microscope (SEM; Figures S8 and S9, Supporting Information). **Figure 3**a shows that T increases from 46.5 to 62.8 μm with the precipitation time from 60 to 105 min, when the experiment condition is the same as that of Figure 2b. After 105 min, the precipitation almost completes; therefore, the increase in T slows down. T can also be tuned by changing the concentration of TA-PEG. T increases from 18.3 to 126.6 μm with the increment in the concentration of TA-PEG from 5 to 20 mg mL^{-1}, when the precipitation time is fixed at 90 min (Figure 4b).

2.3. High Binding Affinity to Various Substrates and Easy Erasure

Besides PS, the TA-PEG coatings can also be facilely fabricated on other substrates without the need of special pretreatments (Figure S10, Supporting Information). Stainless steel, glass, polydimethylsiloxane, and polyethylene terephthalate (PET) were selected as representative inorganic and organic substrates for coating. Owing to the high binding affinity of TA to various surfaces,[37–39] the coatings bond tightly to all these substrates and cannot be peeled off by an adhesive Scotch tape for at least ten times. **Figure 4**a,b shows that the cross-section of the coating hardly changes after peeled with an adhesive Scotch tape for ten times. To characterize the adhesion force, another substrate of the same material was placed atop the wet coating; after drying, the load–displacement curves of coating adhesion to these substrates were measured (Figure 4d). The adhesion strengths of the TA-PEG coatings to stainless steel, glass, PS, and PET substrates are 0.76 ± 0.05, 0.59 ± 0.02, 1.08 ± 0.08, and 1.91 ± 0.14 MPa, respectively. These results indicate the university of our method to fabricate coatings with strong adhesion to different substrates. However, the coatings can be easily removed from the substrates if needed, for example, when the damages are too severe or the coatings are contaminated. The TA-PEG coatings can be completely dissolved in 0.01 M NaOH aqueous solution in 10 min, which leads to the ionization of TAs and disruption of the intermolecular hydrogen bonds. **Figure 5**a shows a general coating removal process. TAs dissolved in the alkali solution are fast oxidized[38] making the solution turn yellow. The PET substrate after removing the coating has identical Fourier transform-infrared/attenuated total reflection (FT-IR/ATR) spectrum with the original substrate, indicating no residual TA or PEG is left (Figure 5b).

2.4. Self-Healing Capabilities

The TA-PEG coatings have water-enabled self-healing capacities; the healing process can be observed by SEM or optical microscopy. A cut with ≈50 µm in width was made to the coating with a knife, which penetrated to the surface of PS substrate (**Figure 6**a). After the sample is immersed in water, the cut partially heals after 20 s (Figure 6b) and completely heals within 5 min (Figure 6c) at room temperature. The self-healing process was also observed in situ under an inverted optical microscope (Figure 6d). When a water droplet is dripped on the damaged coating, the cut completely heals within 5 min. In addition, the cut can also totally heal after being exposed to a 100% humidity environment for 30 min at room temperature (Figure S11, Supporting Information) because the coatings are softened with certain fluidity. However, the coatings are stable under humidity less than 93%, in which the coatings are not soft enough to flow under gravity or dewet on the substrate (Figure S12, Supporting Information). Damages on the same area of coating can repeatedly heal at least five times without any observable decline in the self-healing abilities due to the break and formation of hydrogen bonds (Figure S13, Supporting Information). The self-healing mechanism of the TA-PEG coatings is discussed based on the modulus variation at different states. The TA-PEG coatings are significantly softened under water; the Young's modulus of the coatings drops dramatically from 6.4 GPa (the dry state) to 0.89 MPa (the swollen state) (Figure 6e). When the damaged dry coatings are in contact with water or exposed to a moist environment, the hydrogen bonds between TA and PEG are weakened, rendering the coatings with slight fluidity. As a result, the highly swollen and softened coatings can deform and fill the cracks[11,25] and reunite through hydrogen bonding. Then, the coatings adjust themselves to be smooth and uniform to reduce the surface energy. This process can also be clearly visualized in situ (Figure 6d).

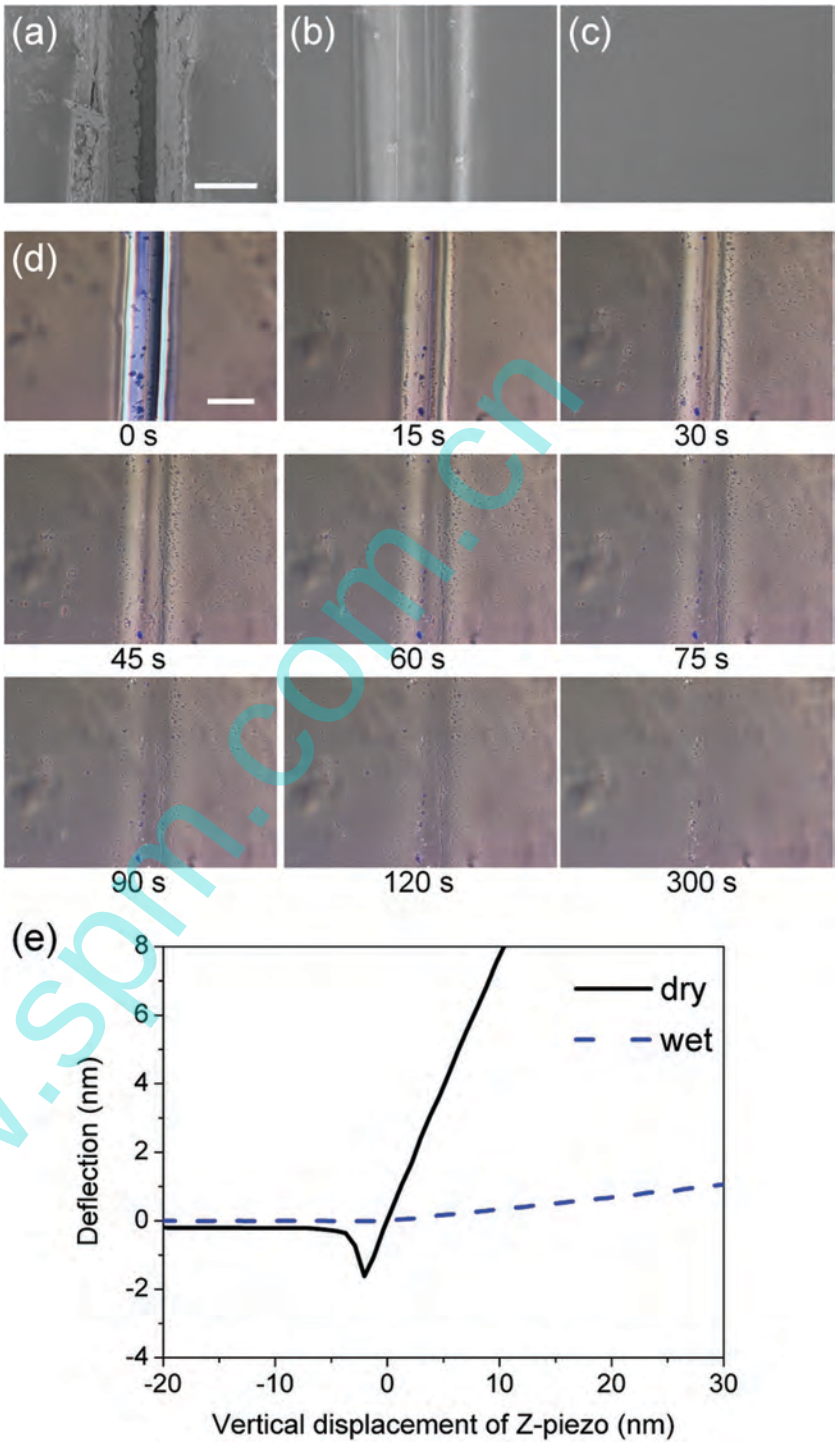

Figure 6. a–c) SEM images of a dry TA-PEG coating damaged with a knife (a), partially or completely healed after being immersed in water for 20 s (b) or 5 min (c), respectively. Scale bar: 50 µm. d) Microscopic images to show the healing of a damaged TA-PEG coating on a PS substrate. A water drop was dripped on the damaged area after 0 s; the morphology change was observed under a microscope in the following 300 s. Scale bar: 100 µm. e) Deflection–displacement loading curves of dry and wet TA-PEG coatings.

2.5. Antioxidant Properties

Besides the water-enabled self-healing capacities, the TA-PEG coatings also possess antioxidant properties because TA is able to scavenge ROS.[38,46] The antioxidant property of TA-PEG coatings was assessed by using 2,2-diphenyl-1-picrylhydrazyl (DPPH) as the model oxidant. 160 µL DPPH methanol solution (3 mg mL^{-1}, containing 50 mg mL^{-1} PEG) was uniformly dripped on PET substrates (1.6 cm^2 area) with or without TA-PEG coatings. PEG in methanol was used to form uniform

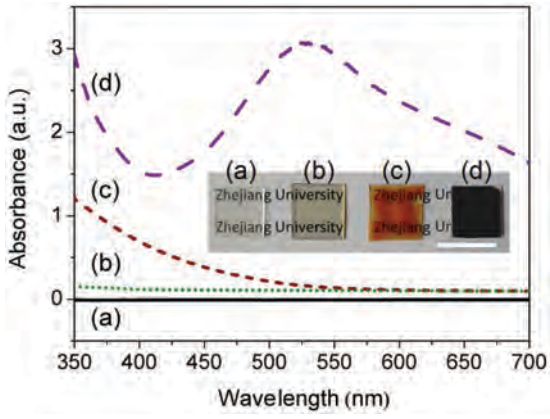

Figure 7. UV–vis spectra of bare and TA-PEG coated PET substrates at different states. a) Bare PET substrates; b) TA-PEG coated PET substrates; c) TA-PEG coated PET substrates dripped with DPPH solution; d) PET substrates dripped with DPPH solution. Insets are digital images of corresponding samples. Scale bar: 1.5 cm.

layers with DPPH on the bare PET substrates. After evaporating the solvent of methanol, UV–vis spectrophotometry was applied to analyze the state of PET substrates with DPPH (**Figure 7**). The virgin TA-PEG coatings on PET substrates are colorless and transparent with only slight visible absorption. Without the coating layers, the PET substrates with DPPH atop are dark purple and show a characteristic absorption peak of DPPH at 515–520 nm.[38,49] In contrast, when the PET substrates have TA-PEG coatings, the purple color of DPPH fades away in ≈10 min; there is no absorption peak at 515–520 nm, indicating DPPH is totally reduced by TA in the coatings. The coatings turn to reddish orange during this process due to the oxidation of TA. This result demonstrates that TA-PEG coatings can protect the substrates from being oxidized before the oxidation of all TA molecules. Besides, these coatings are extremely stable in air. No obvious changes can be observed in the transparency, color (Figure S13l, Supporting Information) and surface morphology (Figure S4b, Supporting Information) after a sample is placed in air at room temperature for over five months.

3. Conclusion

In conclusion, we have presented a universal yet facile method to fabricate transparent water-enabled self-healing coatings on various substrates by the precipitation of TA-PEG complexes in aqueous solution. The coatings are robust after drying, yet swollen and softened under water or in moist environment, resulting in autonomic healing the mechanical damages via rebuilding hydrogen bonds between TA and PEG. Compared with the LBL approach used to fabricate self-healing coatings, our method has advantages in its adaption to various substrates as well as time and cost efficiency; thus obtained coatings can strongly bind to various substrates without pretreatment or modification. However, the coatings can be easily removed from the substrates after being contaminated or damaged too severely. Furthermore, TA endows the coatings with the capacity to protect the substrates against being oxidized, which can be used to protect biomaterials, precision instruments, etc. The method via precipitating soft complexes should be suitable to other systems to fabricate coatings with additional functionalities.

4. Experimental Section

Materials: Tannic acid (TA) and 2,2-diphenyl-1-picrylhydrazyl (DPPH) were purchased from Sigma-Aldrich (USA) and used as received. Analytical-grade NaCl, KNO_3, methanol, and polyethylene glycol (PEG) with weight-average molecular weight (M_w) of 0.4, 1, 2, 4, 10, and 20 kDa were all obtained from Sinopharm Chemical Reagent Limited Corporation (China). Ultrapure water (18.2 MΩ) was produced from an ELGA Lab Water system (France). All the substrates used in this work were cleaned by subsequent sonication in 2-propanol and ultrapure water for 20 min, respectively, followed by washing with ultrapure water for three times and drying.

Fabrication of TA-PEG Coatings: In general, clean substrates for coatings were placed on the bottom of PS 12-well plates. The basal area of each well is about 4.15 cm^2. Then, TA and PEG aqueous solutions (each one 1.5 mL, 10 mg mL^{-1}, containing 0.5 M NaCl) were poured and vigorously mixed in each well. Thus formed emulsions were stewed for 90 min for the precipitation and coalescence of the TA-PEG complexes on the substrates. Finally, uniform coatings were formed on the substrates, which were taken out and dried at room temperature. As a consequence, mechanically robust coatings were obtained. Following a similar process, the concentration of PEG and TA, precipitation time, molecular weight of PEG, and substrate materials were varied to control the coating properties.

Characterization: Laser diffraction measurements (Beckman Coulter, LS-230 Coulter, USA) were used to analyze the size distribution of TA-PEG complexes in the emulsions. Inverted optical microscope (Eclipse TE2000, Nikon, Tokyo, Japan), equipped with a highly sensitive CCD camera (ORCA-ER, Hamamatsu Photonics, Shizuoka, Japan) was used to in situ observe the formation of TA-PEG coatings. In situ observation of the healing was also performed by utilizing this microscope after dripping a droplet of water on the damaged dry coatings. In addition, field emission scanning electron microscopy (FESEM, Hitachi, S4800, Japan) was used to observe the morphology of damaged coatings and the self-healing process; it was also used to measure the coating thickness prepared at different conditions on PS substrates. All samples were sputtered with ≈5 nm gold nanoparticles before SEM observation. FT-IR/ATR (Nicolet6700, USA) was used to analyze the chemical compositions of the TA-PEG coatings before and after removed from the PET substrates.

Lap Shear Experiment: The lap shear tests were performed with electromechanical testing systems (Instron 5540A, Instron Corporation, USA) in air at ambient temperature with a relative humidity of ≈60%. TA-PEG coatings were fabricated on various substrates (5 × 40 mm^2). Then another piece of the same substrate was adhered to the coating surface with a contact area of 5 × 5 mm^2. Subsequently, the samples were dried under room temperature. The adhesion force was measured by a tensile test. The adhered substrates were held by the two mechanical chucks and loaded to failure at 1 mm min^{-1}. Based on the fracture force, the failure stress was obtained, which reflects the bonding strength of the coatings on the substrates.

Deflection–Displacement Loading Curve Measurement: Atomic force microscope (AFM, CSPM 5500, Being Nano-Instruments, Ltd., China) was used to measure the Young's modulus of the TA-PEG coatings at different conditions. Deflection–displacement loading curves of TA-PEG coatings were measured in about 40% relative humidity environment for dry condition. As for wet condition, TA-PEG coatings were immersed in water for 1 min and then taken out to measure the loading curves in air. Calculation of Young's moduli of the coatings is demonstrated in the Supporting Information.

Self-Healing Tests: Cuts about 50 μm in width were made by a knife, which penetrated to the PS substrates. Then the coatings were immersed

in water for 20 s or 5 min for partial or complete healing of the damages, respectively. The healing process was observed by using inverted optical microscopy and SEM. The healing of coatings can also be accomplished by keeping the sample in a 100% humidity environment, which was achieved by sealing 40 mL deionized water in a 200 mL beaker for 3 h. TA-PEG coatings were placed in a small PS culture dish, which was floated on the water in the beaker. After 30 min, the samples were taken out and dried before SEM observation.

Stability Tests under High Humidity: PET substrates with TA-PEG coatings were vertically placed in a sealed container with ≈93% humidity, which was maintained by keeping a saturated KNO_3 aqueous solution inside. After 24 h, the samples were taken out and observed under an optical microscopy.

Antioxidant Tests: 160 µL of 3 mg mL^{-1} DPPH methanol solution (containing 50 mg mL^{-1} PEG (M_w = 1 kDa)) was uniformly dripped on PET substrates (1.6 cm^2 area) with or without TA-PEG coatings. After drying, the as-treated PET sheets were subjected to UV–visible spectrophotometry, with an ultraviolet spectrophotometer (UV 2450, Shimadzu, Japan) from 350 to 700 nm in a transmission mode. Digital images were also obtained under this condition.

Supporting Information

Supporting Information is available from the Wiley Online Library or from the author.

Acknowledgements

This work was supported by the National Natural Science Foundation of China under Grant No. 21534009. The authors would like to thank Tingting Chen for her kind advice on the lap shear tests.

Received: February 26, 2016
Revised: April 14, 2016
Published online:

[1] Y. Yang, M. W. Urban, *Chem. Soc. Rev.* **2013**, *42*, 7446.
[2] X. Chen, M. A. Dam, K. Ono, A. Mal, H. Shen, S. R. Nutt, K. Sheran, F. Wudl, *Science* **2002**, *295*, 1968.
[3] a) Y. Amamoto, J. Kamada, H. Otsuka, A. Takahara, K. Matyjaszewski, *Angew. Chem.* **2011**, *123*, 1698; b) Y. Amamoto, J. Kamada, H. Otsuka, A. Takahara, K. Matyjaszewski, *Angew. Chem. Int. Ed.* **2011**, *50*, 1660.
[4] C. J. Hansen, W. Wu, K. S. Toohey, N. R. Sottos, S. R. White, J. A. Lewis, *Adv. Mater.* **2009**, *21*, 4143.
[5] T.-S. Wong, S. H. Kang, S. K. Y. Tang, E. J. Smythe, B. D. Hatton, A. Grinthal, J. Aizenberg, *Nature* **2011**, *477*, 443.
[6] N. H. Andersen, M. J. Harrington, H. Birkedal, B. P. Lee, P. B. Messersmith, K. Y. C. Lee, J. H. Waite, *Proc. Natl. Acad. Sci. USA* **2011**, *108*, 2651.
[7] P. Cordier, F. Tournilhac, C. S-Ziakovic, L. Leibler, *Nature* **2008**, *451*, 977.
[8] B. K. Ahn, D. W. Lee, J. N. Israelachvili, J. H. Waite, *Nat. Mater.* **2014**, *13*, 867.
[9] S. R. White, N. R. Sottos, P. H. Geubelle, J. S. Moore, M. R. Kessler, S. R. Sriram, E. N. Brown, S. Viswanathan, *Nature* **2001**, *409*, 794.
[10] K. S. Toohey, N. R. Sottos, J. A. Lewis, J. S. Moore, S. R. White, *Nat. Mater.* **2007**, *6*, 581.
[11] a) X. Wang, F. Liu, X. Zheng, J. Sun, *Angew. Chem.* **2011**, *123*, 11580; b) X. Wang, F. Liu, X. Zheng, J. Sun, *Angew. Chem. Int. Ed.* **2011**, *50*, 11378.
[12] J.-H. Park, P. V. Braun, *Adv. Mater.* **2010**, *22*, 496.
[13] S. H. Cho, S. R. White, P. V. Braun, *Adv. Mater.* **2009**, *21*, 645.
[14] D. G. Shchukin, H. Möhwald, *Small* **2007**, *3*, 926.
[15] a) C. E. Diesendruck, N. R. Sottos, J. S. Moore, S. R. White, *Angew. Chem.* **2015**, *127*, 10572; b) C. E. Diesendruck, N. R. Sottos, J. S. Moore, S. R. White, *Angew. Chem. Int. Ed.* **2015**, *54*, 10428.
[16] A. P. E. Kahn, N. R. Sottos, S. R. White, J. S. Moore, *J. Am. Chem. Soc.* **2010**, *132*, 10266.
[17] M. M. Caruso, D. A. Davis, Q. Shen, S. A. Odom, N. R. Sottos, S. R. White, J. S. Moore, *Chem. Rev.* **2009**, *109*, 5755.
[18] P. Froimowicz, H. Frey, K. Landfester, *Macromol. Rapid Commun.* **2011**, *32*, 468.
[19] B. Yang, J. Liu, H. Zheng, S. X.-A. Zhang, *Chin. J. Chem.* **2013**, *31*, 1483.
[20] Y. Li, S. Chen, M. Wu, J. Sun, *ACS Appl. Mater. Interfaces* **2014**, *6*, 16409.
[21] S. Bode, L. Zedler, F. H. Schacher, B. Dietzek, M. Schmitt, J. Popp, M. D. Hager, U. S. Schubert, *Adv. Mater.* **2013**, *25*, 1634.
[22] D. V. Andreeva, D. Fix, H. Möhwald, D. G. Shchukin, *Adv. Mater.* **2008**, *20*, 2789.
[23] J. A. Syed, S. Tang, H. Lu, X. Meng, *Colloid Surf., A* **2015**, *476*, 48.
[24] Y. Dou, A. Zhou, T. Pan, J. Han, M. Wei, D. G. Evans, X. Duan, *Chem. Commun.* **2014**, *50*, 7136.
[25] a) A. B. South, L. A. Lyon, *Angew. Chem.* **2010**, *122*, 779; b) A. B. South, L. A. Lyon, *Angew. Chem. Int. Ed.* **2010**, *49*, 767.
[26] S. J. García, H. R. Fischer, S. Zwaag, *Prog. Org. Coat.* **2011**, *72*, 211.
[27] D. Chen, M. Wu, B. Li, K. Ren, Z. Cheng, J. Ji, Y. Li, J. Sun, *Adv. Mater.* **2015**, *27*, 5882.
[28] Y. Wang, T. Li, S. Li, R. Guo, J. Sun, *ACS Appl. Mater. Interfaces* **2015**, *7*, 13597.
[29] Y. Li, S. Chen, M. Wu, J. Sun, *Adv. Mater.* **2012**, *24*, 4578.
[30] X. Wang, Y. Wang, S. Bi, Y. Wang, X. Chen, L. Qiu, J. Sun, *Adv. Funct. Mater.* **2014**, *24*, 403.
[31] C. W. Park, A. B. South, X. Hu, C. Verdes, J.-D. Kim, L. A. Lyon, *Colloid Polym. Sci.* **2011**, *289*, 583.
[32] X. Huang, M. J. Bolen, N. S. Zacharia, *Phys. Chem. Chem. Phys.* **2014**, *16*, 10267.
[33] U. Manna, D. M. Lynn, *Adv. Mater.* **2013**, *25*, 5104.
[34] E. V. Skorbab, D. V. Andreeva, *Polym. Chem.* **2013**, *4*, 4834.
[35] J. C. Gaulding, M. W. Spears Jr., L. A. Lyon, *Polym. Chem.* **2013**, *4*, 4890.
[36] M. W. Spears Jr., E. S. Herman, J. C. Gaulding, L. A. Lyon, *Langmuir* **2014**, *30*, 6314.
[37] H. Ejima, J. J. Richardson, K. Liang, J. P. Best, M. P. Koeverden, G. K. Such, J. Cui, F. Caruso, *Science* **2013**, *341*, 154.
[38] a) T. S. Sileika, D. G. Barrett, R. Zhang, K. H. A. Lau, P. B. Messersmith, *Angew. Chem.* **2013**, *125*, 10966; b) T. S. Sileika, D. G. Barrett, R. Zhang, K. H. A. Lau, P. B. Messersmith, *Angew. Chem. Int. Ed.* **2013**, *52*, 10766.
[39] X. Zhang, P.-F. Ren, H.-C. Yang, L.-S Wan, Z.-K. Xu, *Appl. Surf. Sci.* **2016**, *360*, 291.
[40] H. Lee, S. M. Dellatore, W. M. Miller, P. B. Messersmith, *Science* **2007**, *318*, 426.
[41] H.-C. Yang, K.-J. Liao, H. Huang, Q.-Y. Wu, L.-S. Wan, Z.-K. Xu, *J. Mater. Chem. A* **2014**, *2*, 10225.
[42] Y. Lv, H.-C. Yang, H.-Q. Liang, L.-S. Wan, Z.-K. Xu, *J. Membr. Sci.* **2015**, *476*, 50.
[43] W.-Z. Qiu, H.-C. Yang, L.-S. Wan, Z.-K. Xu, *J. Mater. Chem. A* **2015**, *3*, 14438.
[44] I. E. Unal, S. A. Sukhishvili, *Macromolecules* **2008**, *41*, 3962.
[45] K. Kim, M. Shin, M.-Y. Koh, J. H. Ryu, M. S. Lee, S. Hong, H. Lee, *Adv. Funct. Mater.* **2015**, *25*, 2402.
[46] T. Bahorun, V. Neergheen-Bhujun, N. A. Toolsee, J. Somanah, A. Luximon-Ramma, O. I. Aruoma, *Tea in Health and Disease Prevention*, Academic Press, New York **2013**, p. 361.
[47] M. Radmacher, M. Fritz, C. M. Kacher, J. P. Cleveland, P. K. Hansma, *Biophys. J.* **1996**, *70*, 556.
[48] S. L. Crick, F. C.-P. Yin, *Biomech. Model. Mech.* **2007**, *6*, 199.
[49] Y. C. Jiménez, M. V. G.-Moreno, J. M. Igartuburu, C. G. Barroso, *Food Chem.* **2014**, *165*, 198.

